Developmental Cognitive Neuroscience 32 (2018) 43–54

Contents lists available at ScienceDirect

Developmental Cognitive Neuroscience

journal homepage: www.elsevier.com/locate/dcn

The Adolescent Brain Cognitive Development (ABCD) study: Imaging acquisition across 21 sites

B.J. Casey[a,b,*], Tariq Cannonier[a], May I. Conley[a,b], Alexandra O. Cohen[b], Deanna M. Barch[c], Mary M. Heitzeg[f], Mary E. Soules[f], Theresa Teslovich[b], Danielle V. Dellarco[b], Hugh Garavan[g], Catherine A. Orr[g], Tor D. Wager[h], Marie T. Banich[h], Nicole K. Speer[h], Matthew T. Sutherland[i], Michael C. Riedel[i], Anthony S. Dick[i], James M. Bjork[j], Kathleen M. Thomas[k], Bader Chaarani[g], Margie H. Mejia[l], Donald J. Hagler Jr.[l], M. Daniela Cornejo[l], Chelsea S. Sicat[l], Michael P. Harms[d], Nico U.F. Dosenbach[e], Monica Rosenberg[a], Eric Earl[m], Hauke Bartsch[l], Richard Watts[g], Jonathan R. Polimeni[n], Joshua M. Kuperman[l], Damien A. Fair[m], Anders M. Dale[l], the ABCD Imaging Acquisition Workgroup[1]

[a] Department of Psychology, Yale University, United States
[b] Sackler Institute for Developmental Psycholobiology, Weill Cornell Medical College, United States
[c] Departments of Psychological & Brain Sciences and Psychiatry, Washington University, St. Louis, United States
[d] Department of Psychiatry, Washington University, St. Louis, United States
[e] Department of Pediatric Neurology, Washington University, St. Louis, United States
[f] Department of Psychiatry, University of Michigan, United States
[g] Departments of Psychiatry and Radiology, University of Vermont, United States
[h] Department of Psychology & Neuroscience, University of Colorado, Boulder, United States
[i] Departments of Physics and Psychology, Florida International University, United States
[j] Department of Psychiatry, Virginia Commonwealth University, United States
[k] Institute of Child Development, University of Minnesota, United States
[l] Center for Human Development, Departments of Neuroscience and Radiology, University of California, San Diego, United States
[m] Behavioral Neuroscience and Psychiatry, Oregon Health State University, United States
[n] Athinoula A. Martinos Center for Biomedical Imaging, Department of Radiology, Harvard Medical School, Massachusetts General Hospital, United States

ARTICLE INFO

Keywords:
Addiction
Adolescence
Development
Impulsivity
Memory
Reward

ABSTRACT

The ABCD study is recruiting and following the brain development and health of over 10,000 9–10 year olds through adolescence. The imaging component of the study was developed by the ABCD Data Analysis and Informatics Center (DAIC) and the ABCD Imaging Acquisition Workgroup. Imaging methods and assessments were selected, optimized and harmonized across all 21 sites to measure brain structure and function relevant to adolescent development and addiction. This article provides an overview of the imaging procedures of the ABCD study, the basis for their selection and preliminary quality assurance and results that provide evidence for the feasibility and age-appropriateness of procedures and generalizability of findings to the existent literature.

1. Introduction

Neuroimaging provides a tool for examining the biological development of the human brain in vivo. A primary aim of the ABCD study is to track human brain development from childhood through adolescence to determine biological and environmental factors that impact or alter developmental trajectories. This landmark study is recruiting and following approximately 10,000 9–10 year olds across the United States. Longitudinal measures of brain structure and function are a central focus of the study. The ABCD Imaging Acquisition Workgroup https://abcdstudy.org/scientists-workgroups.html selected, optimized and harmonized measures and procedures across all 21 ABCD sites. This article provides the basis for, and overview of, the ABCD imaging procedures and preliminary quality assessments that indicate the

* Corresponding author at: Department of Psychology, Yale University, 2 Hillhouse Ave, New Haven, CT, 06511, United States.
E-mail address: BJ.Casey@Yale.edu (B.J. Casey).
[1] https://abcdstudy.org/scientists-workgroups.html.

https://doi.org/10.1016/j.dcn.2018.03.001
Received 26 May 2017; Received in revised form 29 January 2018; Accepted 2 March 2018
Available online 14 March 2018

developmental appropriateness of the protocol for 9 and 10 year olds.

Numerous Big Data studies have emerged around the world (Rosenberg et al., under review 2018) that assess human brain function and structure with magnetic resonance imaging (MRI) of the developing mind and brain. The ABCD study capitalizes on the advancing technologies in structural and functional MRI of these studies, especially from the Human Connectome Project (HCP; https://www.humanconnectome.org) and the Pediatric Imaging, Neurocognition, and Genetics (PING) Study (http://pingstudy.ucsd.edu, Jernigan et al., 2016) and components of the IMAGEN study (www.imagen-europe.com; Schumann et al., 2010) that combines brain imaging and genetics to examine adolescent development and human behavior.

Building upon the efforts of these Big Data studies has led to the establishment of an optimized MRI acquisition protocol to measure brain structure and function that is harmonized to be compatible across three 3 tesla (T) scanner platforms: Siemens Prisma, General Electric 750 and Phillips at 21 sites. The protocol includes 3D T1- and 3D T2 weighted images, and diffusion weighted images for measures of brain structure; and resting state and task-based functional MRI for measures of brain function.

ABCD task-based functional assessment of the brain consists of three tasks: the Monetary Incentive Delay (MID) task (Knutson et al., 2000), the Stop Signal task (SST, Logan, 1994b) and an emotional version of the n-back task (EN-back, Cohen et al., 2016b; Barch et al., 2013). Together these tasks measure 6 of the original National Institute**s** of Health's Collaborative Research on Addiction at NIH (**CRAN**) Request for Applications (RFA)-mandated domains of function: reward processing, motivation, impulsivity, impulse control, working memory and emotion regulation. Each of the 6 behavioral domains measured by the ABCD fMRI tasks are highlighted in Table 1 indicating behavioral domain, task, processes and neural correlates.

2. ABCD materials and methods

An important motivating factor for the study is to identify developmental trajectories and neural signatures for adolescent mental health. To ensure that the study has the statistical power to characterize these different developmental trajectories, an aim of the study is for approximaetely 50% of the sample to consist of children who show early signs of externalizing and internalizing symptoms. The sample and overall design of the ABCD study are described by Garavan et al., Loeber et al. and Volkow et al. this issue. Also, see Clark et al. (this issue) for details on ethical considerations of the study. The imaging protocol, procedures, and tasks are described in detail below with emphasis on harmonization of procedures across the 21 ABCD sites.

2.1. Equipment and software

2.1.1. Scanner and head coil

The ABCD imaging protocol is harmonized for three 3T scanner platforms (*Siemens Prisma, General Electric (GE) 750 and Philips)* and use of multi-channel coils capable of multiband echo planar imaging (EPI) acquisitions, using a standard adult-size coil. **T**he decision to use a standard head coil for each scanner platform across ages rather than using nonstandard customized coils was threefold. First, 9 and 10 year olds have brains that are typically between 90 and 95% of adult brain size. There is empirical evidence for the feasibility of using a common stereotactic space for this age as that used for adults (Burgund et al., 2002; Kang et al., 2003). Second, the use of custom coils for each age would introduce significant challenges to the analysis with the coil being confounded with age. Third, custom coils require the manufacturer to produce and provide customization of coils and connectors that was not feasible to obtain across all sites during the first year of optimization and harmonization of the scan protocol. It has been important throughout the design of the ABCD study to coordinate with the vendors to ensure stability of the hardware from the start of the study in September 2016 and over the course of this 10-year study.

2.1.2. Stimulus presentation and response collection

The task-based fMRI scans require special stimulus presentation and response collection equipment and software. All ABCD fMRI tasks are currently programmed in E-Prime Professional 2.0 versions 2.0.10.356 or later and work reliably for PC Windows 8.1 or earlier. The tasks and stimuli are available for download at: http://fablab.yale.edu/page/assays-tools. The response collection device is harmonized for precision in response latency across all tasks and all sites with a *Current Designs* 2-button box. The tasks are programed to accept input from the dominant hand (left or right). Visual display and auditory delivery equipment are not harmonized given the variability in scanner and control room set-up across sites and no mandate for precise visual or auditory resolution for the fMRI tasks was imposed. Sites use rear projection or goggles for visual display and a variety of head phone/ear bud devices. Tasks are programmed to accommodate these various set-ups across sites.

3. ABCD scan protocol

The ABCD neuroimaging protocol is depicted in Fig. 1. The final ABCD protocol was based in part on a multi-site (12 ABCD sites) pilot study of a convenience sample of 67 children and teens from varied household incomes and racial and ethnic backgrounds and included individuals at risk for substance abuse and mental health problems. Over 30 of these children provided imaging pilot data. These data showed no more fatigue, as measured by poorer fMRI task performance and self-report, when completing the scan protocol in one session versus two, or when administering the fMRI tasks at the beginning of the scan session versus at the end. Thus, scanning occurs in either 1 or 2 sessions. Varying the number of scan sessions provides added flexibility for sites that have constraints in scanner access and aids in accommodating constraints that ABCD families may have in their schedules, etc. In addition to the pilot data, further evidence of the feasibility of the ABCD imaging protocol for 9–10 year olds is indicated by the high completion of scans for the first approximately 1000 subjects. These

Table 1
Domains of function measured by the ABCD fMRI tasks.

RFA Domain	Task	Processes	Neural Correlates
Reward Processing	Monetary Incentive Delay	Anticipation and outcome of reward and loss	Ventral striatum, orbitofrontal and medial prefrontal cortex
Motivation	Monetary Incentive Delay- response to cue	Anticipation of responding for outcome	Ventral striatum and ventromedial prefrontal cortex
Impulsivity	Stop Signal Task: Failed Stops	Impulsivity, error monitoring	Dorsal striatum, anterior cingulate cortex
Impulse Control	Stop Signal Task: Correct Stops	Impulse control, conflict monitoring and resolution	Ventroateral prefrontal cortex, anterior cingulate cortex
Memory	Emotional n-back: 2-back vs 0-back, Recognition task: old vs new items	Working memory, encoding, retrieval, forgetting, recognition	Dorsolateral prefrontal, parietal and premotor cortex, hippocampus, parahippocampus
Emotion Regulation	Emotional n-back: Fearful or happy vs neutral faces	Emotion regulation and reactivity	Dorsolateral, ventrolateral and ventromedial prefrontal cortex, amygdala, ventral striatum

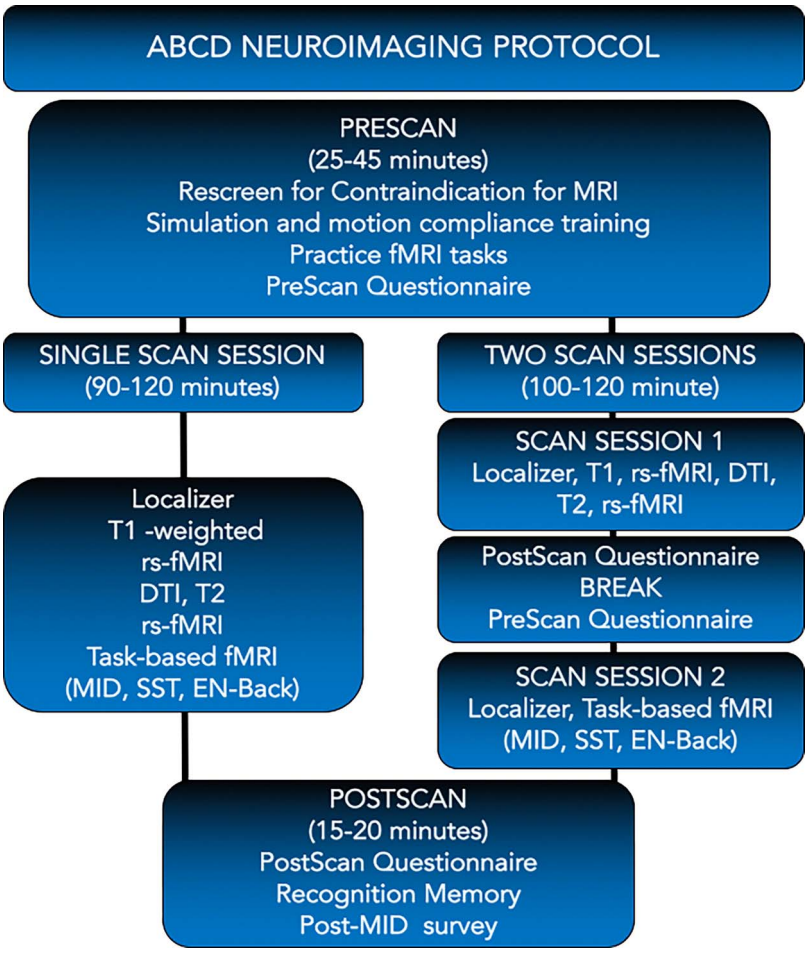

Fig. 1. ABCD Neuroimaging Protocol.

data show that 99% of the enrolled subjects completed the 3D T1-weighted scan. The remaining scans varied in completion from 88 to 98% (rs-fMRI = 98%, diffusion = 97%, 3D T2 = 96%, MID = 91%. SST = 89% and the EN-back = 88%). Thus, completion of all scan types across sites is at nearly 90%.

3.1. Ordering of scans

The scan session consists of a fixed order of scan types that begin with a localizer, acquisition of 3D T1-weighted images, 2 runs of resting state fMRI, diffusion weighted images, 3D T2-weighted images, 1–2 more runs of resting state fMRI (see motion detection below for when to acquire 1 versus 2 additional runs) and the task-based fMRI. Although the order of scans across subjects is fixed as shown in Fig. 1, the order and version of the 3 fMRI tasks (MID, SST and EN-back) are randomized across subjects. The decision to randomize the order of fMRI tasks across subjects was based in part on these scans being the most cognitively demanding on the child. Whereas, the structural and resting state scans simply require the child to relax and watch a movie or look in the general direction of a fixation crosshair, the fMRI tasks require anticipation and outcome of rewards and losses, impulse control, emotion regulation, memory and action on the part of the child (see Table 1. *Domains of function measured by the ABCD fMRI tasks*). Also, negative affective processes can diminish cognitive performance (Cohen et al., 2016a) and performing a demanding cognitive task has been associated with diminished performance on subsequent tasks (Baumeister et al., 1998). We therefore randomized the order of tasks across subjects to help control for these effects.

Likewise, we randomized the order of trials within tasks to help control for the effects of different processing demands of one trial on a subsequent trial. Based on simulations, 12 pseudorandom trial sequences optimized to minimize variance in activation parameter estimates were selected for tasks with event related designs (MID and SST). This allows investigators to assess generalizability over task variants (trial sequences) and control for sequence if necessary. The EN-back was programmed as a block design given time constraints, number and level of factors (4 stimulus types, 2 memory loads) and the need for instructed task switching between memory load conditions.

Finally, the random assignment of a given order and version of tasks to a subject at baseline is held constant across longitudinal scans to minimize within-subject variability and enhance the ability to test key ABCD specific aims that focus on individual differences in developmental trajectories. In addition, participants within a family (e.g., twin pairs/siblings) receive the same order and version of the fMRI tasks to minimize within-family variability for testing heritability and genetic effects. Details of the imaging protocol are described in detail below for each component: pre-scan, scan and post-scan.

3.2. Pre-scan assessments and training

3.2.1. MR screening

Participants complete an MR screening questionnaire for any contraindication for an MRI (e.g., braces, pacemakers, and other metal in the body including piercings, medical screw, pins, etc.). This MR screening occurs three times: during initial recruitment, at scheduling, and just prior to the scan.

3.2.2. Simulation and motion compliance training

Before the scan, participants are desensitized to the scanner environment with a simulator. Simulation occurs in dedicated mock scanners with prerecorded scanner sounds and/or collapsible play tunnels the diameter of the scanner bore (55–60 mm). Because head motion is a significant problem for pediatric imaging, behavioral shaping techniques are used for motion compliance training (Epstein et al., 2007). Commercial simulators, or Wii devices affixed to the child's head (see Supplemental Text) monitor head motion and provide feedback to the child. After simulation and motion compliance, the participants practice the three fMRI tasks to be sure they understand the instructions and are familiarized with the response collection device.

3.2.3. Arousal questionnaire

Immediately prior to scanning, the participant is given a restroom break and then administered a questionnaire on his/her current state of arousal (Supplemental Table 1). This questionnaire is administered again at the end of the scan (see Post Scan Assessments). Earplugs are inserted, and the child is placed on the scanner bed. Physiologic noise is measured with a respiratory belt placed around the child's stomach to measure breathing rate and a pulse oximeter placed on the child's non-dominate pointer finger to measure heart rate. To minimize motion, the head is stabilized with foam padding around head phones/earbuds. The technologist localizes the head position, ensures that the child can fully view the screen, and has the child test the response box buttons. As the scanner table moves to the center of the scanner bore, a child appropriate movie is played and the staff makes sure the child can see and hear it.

3.3. Scan session

A child friendly movie is turned on as the child enters the scanner and remains on during acquisition of the localizer and 3D T1 scans and is also played during the 3D T2 and diffusion weighted imaging acquisitions. The functional scans include twenty minutes of resting-state data acquired with eyes open and passive viewing of a cross hair. One set of two 5 min runs is acquired immediately after the 3D T1 and another set is acquired after the 3D T2 scans. The task-based fMRI images are completed after the final set of resting state scans, counterbalancing the order of tasks across subjects.

3.3.1. Scanning parameters

The imaging parameters for the 3 three 3T scanner platforms are summarized in Table 2. This protocol is shared, although some platforms require agreements for the research sequences, so that every ABCD site can download the protocol and install it with no need for manual entry of parameters, which reduces the likelihood of human error. Images are acquired in the axial plane rather than the oblique orientation since oblique EPI prescriptions are not supported/recommended by GE and Phillips due to ghosting and the potential for peripheral nerve stimulation as the scan plane gets closer to the coronal plane or the phase encoding direction gets closer to the left-right direction. Scan sequences continue to be optimized and made available as the scanner instrumentation is upgraded and improves (e.g., Siemens Prisma upgrade from version VE11B to VE11C). As the technology and sequences are optimized, human phantoms are being collected on all scanners and all software versions within and between sites to control for these changes.

Each scan type measures unique aspects of brain structure and function. The 3D T1-weighted magnetization-prepared rapid acquisition gradient echo scan is obtained for cortical and subcortical segmentation of the brain. The 3D T2-weighted fast spin echo with variable flip angle scan is acquired for detection and quantification of white matter lesions and cerebral spinal fluid (CSF). The high angular resolution diffusion imaging (HARDI) scan, with multiple b-values, and fast integrated B_0 distortion correction (Reversed polarity gradient (RPG) method, Holland et al., 2009; Treiber et al., 2016), is acquired for segmentation of white matter tracts and measurement of diffusion. Finally, high spatial and temporal resolution simultaneous multi-slice (SMS)/multiband EPI resting-state and task-based fMRI scans, with fast integrated distortion correction, are acquired to examine functional activity and connectivity.

3.3.2. Motion detection and correction

Real-time motion detection and correction for the structural scans are implemented by the ABCD DAIC hardware and software. Specifically, anatomical 3D T1- and 3D T-2 weighted images are collected using prospective motion correction (PROMO) on the GE (White et al., 2010), Volumetric Navigators (vNav) for prospective motion correction and selective reacquisition on the Siemens and when available on the Philips platform (Tisdall et al., 2012).

A real-time head motion monitoring system called FIRMM (fMRI Integrated Real-time Motion Monitor, (www.firmm.us, Dosenbach et al., 2017) collaboratively developed at Washington University, St. Louis and Oregon Health Sciences University is implemented for motion detection in resting state fMRI scans at the Siemens sites. FIRMM allows scanner operators to adjust the scanning paradigm based on a participant's degree of head motion (i.e., the worse the motion, the less usable data and greater the need for more data to be acquired).

Head motion is a significant concern for pediatric imaging and has received significant attention in the domain of rs-fMRI (Fair et al., 2012; Power et al., 2012, 2013; Satterthwaite et al., 2012; Yan et al., 2013a, 2013b; Van Dijk et al., 2012). Preliminary motion data are presented in Fig. 2. Motion-detection, −correction and −prevention training are used to help minimize motion. Preliminary analysis of fframe-to-frame displacement of over 2500 participants during resting-state and task-based fMRI data. are provided in Fig. 2. Mean motion is 0.22 mm during rest (SD = 0.20 mm) and less than 0.29 mm in all tasks (n-back M = 0.28, SD = 0.27; SST M = 0.26, SD = 0.25; MID M = 0.25, SD = 0.23). Before mean motion was computed, data were temporally filtered to remove aliased respiratory signals. Future data releases will include six-parameter motion time courses and optimized measures of overall head motion.

Together, the data are relatively encouraging given the young age of the participants (9–10 years), length of the scan protocol (100–120 min), and that approximately 42% of the sample consists of children who show early signs of externalizing and internalizing symptoms and considered at risk for substance abuse and other mental health problems. See Garavan et al., Loeber et al. and Volkow et al. this issue on the study design, recruitment and screener for children at risk for substance abuse and other disorders.

3.3.3. The fMRI tasks

Specific details for each of the fMRI tasks and preliminary quality assessment and results are provided below. These tasks measure processes relevant to addiction and adolescent development and have shown well-characterized and reliable patterns of brain activity in prior imaging studies (refer to Table 1 for a summary). The three tasks were selected based on the existing literature indicating that they met 6 important criteria: 1) implication in addiction (*validity*); 2) feasibility in developmental studies (*developmentally-appropriate*); 3) well-characterized neural activations (*specificity*); 4) reliable activation over time within subjects (*reliability*); 5) consistent patterns of activity across subjects (*sensitivity*); and 6) leveraging of other complementary developmental imaging initiatives that use similar measures (*generalizability*). The relevant literature supporting these claims are provided in the description of each task.

3.3.3.1. Monetary Incentive Delay Task (MID).

The MID task used in the ABCD study (Knutson et al., 2000; Yau et al. 2012) measures the original CRAN ABCD RFA domains of reward processing, including anticipation and receipt of reward and losses, and trial-by-trial

Table 2
ABCD harmonized imaging scanning parameters for Siemens Prisma, Phillips and GE 750 3T scanners.

Siemens (Prisma VE11B-C)	Matrix	Slices	FOV	% FOV phase	Resolution (mm)	TR (ms)	TE (ms)	TI (ms)	Flip Angle (deg)	Parallel Imaging	MultiBand Acceleration	Phase partial Fourier	Diffusion Directions	b-values	Acquisition Time
T1	256 × 256	176	256 × 256	100%	1.0 × 1.0 × 1.0	2500	2.88	1060	8	2×	Off	Off	N/A	N/A	07:12
T2	256 × 256	176	256 × 256	100%	1.0 × 1.0 × 1.0	3200	565	N/A	Variable	2×	Off	Off	N/A	N/A	06:35
Diffusion	140 × 140	81	240 × 240	100%	1.7 × 1.7 × 1.7	4100	88	N/A	90	Off	3	6/8	96	500 (6-dirs); 1000; (15-dirs) 2000; (15-dirs); 3000 (60-dirs)	07:31
fMRI	90 × 90	60	216 × 216	100%	2.4 × 2.4 × 2.4	800	30	N/A	52	Off	6	Off	N/A	N/A	

Philips (Achieva dStream, Ingenia)	Matrix	Slices	FOV	% FOV phase	Resolution (mm)	TR (ms)	TE (ms)	TI (ms)	Flip Angle (deg)	Parallel Imaging	MultiBand Acceleration	Half Scan Factor	Diffusion Directions	b-values	Acquisition Time
T1	256 × 256	225	256 × 240	93.75%	1.0 × 1.0 × 1.0	6.31	2.9	1060	8	1.5 × 2.2	Off	N/A	N/A	N/A	05:38
T2	256 × 256	256	256 × 256	100%	1.0 × 1.0 × 1.0	2500	251.6	N/A	90	1.5 × 2.0	Off	N/A	N/A	N/A	02:53
Diffusion	140 × 140	81	240 × 240	100%	1.7 × 1.7 × 1.7	5300	89	N/A	78	Off	3	0.6	96	500 (6-dirs); 1000; (15-dirs) 2000; (15-dirs); 3000 (60-dirs)	09:14
fMRI	90 × 90	60	216 × 216	100%	2.4 × 2.4 × 2.4	800	30	N/A	52	Off	6	0.9	N/A	N/A	

GE (MR750, DV25-26)	Matrix	Slices	FOV	% FOV phase	Resolution (mm)	TR (ms)	TE (ms)	TI (ms)	Flip Angle (deg)	Parallel Imaging	MultiBand Acceleration	Phase partial Fourier	Diffusion Directions	b-values	Acquisition Time
T1	256 × 256	208	256 × 256	100%	1.0 × 1.0 × 1.0	2500	2	1060	8	2×	Off	Off	N/A	N/A	06:09
T2	256 × 256	208	256 × 256	100%	1.0 × 1.0 × 1.0	3200	60	N/A	Variable	2×	Off	Off	N/A	N/A	05:50
Diffusion	140 × 140	81	240 × 240	100%	1.7 × 1.7 × 1.7	4100	81.9	N/A	77	Off	3	5.5/8	96	500 (6-dirs); 1000; (15-dirs) 2000 (15-dirs); 3000 (60-dirs)	07:30
fMRI	90 × 90	60	216 × 216	100%	2.4 × 2.4 × 2.4	800	30	N/A	52	Off	6	Off	N/A	N/A	

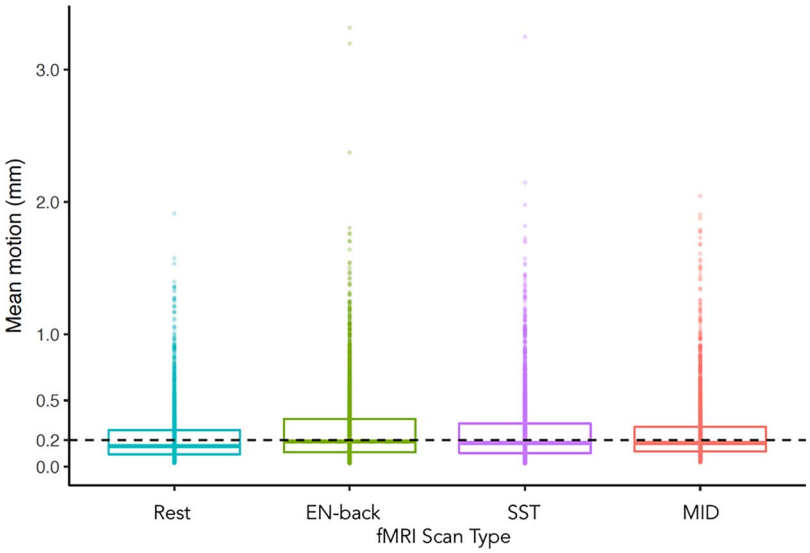

Fig. 2. Preliminary distribution of head motion during resting-state and task-based fMRI scans. Box plots show the distribution of average frame-to-frame displacement during resting-state and emotion (E) N-back, stop-signal task (SST), and monetary incentive delay (MID) task runs from participants with all four scan types (n = 2536). The lower and upper box hinges correspond to the 25th and 75th percentiles; horizontal lines show median values; and dots represent individual participants.

motivation in speeded responses to win or avoid loss (Fig. 2). The MID task is a robust activator of the ventral striatum, demonstrating validity as probe of reward responding (Knutson et al., 2000). This task is sensitive to developmental (Bjork et al. 2004, 2010; Heitzeg et al., 2014) and addiction-related effects (Andrews et al., 2011; Balodis and Potenza, 2015; Beck et al., 2009; Villafuerte et al., 2012; Wrase et al., 2007; Yau et al., 2012) and has good within-subject reliability over time (Villafuerte et al., 2014).

Each trial of the MID task begins with an incentive cue (2000 ms) of five possible trial types (Win $.20, Win $5, Lose $.20, Lose $5, $0-no money at stake) and is followed by a jittered anticipation event (1500–4000 ms). Next, a variable target (150–500 ms) appears during which the participant responds to either win money or avoid losing money. This target event is followed by a feedback message informing the participant of the outcome of the trial. The duration of the feedback is calculated as 2000 ms minus the target duration. The task consists of twelve optimized trial orders of the task (2 runs each). Each run consists of 50 contiguous trials (10 per trial type) presented in pseudorandom order and lasts 5:42.

Task performance is individualized with the initial response target duration based on the participant's performance during a practice session prior to scanning. Performance is calculated as the average reaction time (RT) on correct trials plus two standard deviations. To reach a 60% accuracy rate, the task difficulty is adjusted over the course of the task after every third incentivized trial based on the overall accuracy rate of the previous six trials. If the participant's accuracy falls below the target accuracy level, the duration of the target is lengthened. If the participant's accuracy is above the target accuracy level, the target duration is shortened. Participants gain an average of $21 and all subjects are given at least $1 regardless of performance to maintain motivation during the scan protocol. Hits, RT and monetary payout are calculated (Fig. 3).

For the MID task, the following primary conditions are modeled: reward vs. no money anticipation, loss vs no money anticipation, reward positive feedback vs reward negative feedback, loss positive feedback vs loss negative feedback. Each participant receives 40 reward and loss anticipation trials and 20 no money anticipation trials. For feedback, the adaptive algorithm results in 24 positive feedback trials (for both reward and loss) and 16 negative feedback trials (for both reward and loss) on average.

Preliminary behavioral data from the MID task (n = 965) suggest that the experimental manipulation to maintain hit rates at close to 60% is working. Average hit rates are between 50 and 60% and these rates are maintained across experimental runs (see Fig. 4a). As reported in the literature (Bjork et al., 2010), the average hit rate is slightly higher for reward (59%) and loss trials (54%) than for neutral trials (49%). Reaction times appear relatively stable across runs and conditions. Finally, as anticipated, participants earned on average $21.43 with consistent payoff amounts across experimental runs of $10.56 and $10.87. With age, it will be important to examine variation in response latencies on win and loss trials relative to neutral ones to assess development effects.

Preliminary examination of the MID imaging data look promising. Fig. 4b depicts signed effect sizes (Cohen's d) for the contrast of rewarded trials versus failed trials (n = 856). These images show the expected pattern of increased activity in the ventral striatal striatum and medial prefrontal cortex to reward (Fig. 4b). It will be important to examine how these patterns change and differ for children at risk for substance abuse across development.

3.3.3.2. The stop signal task (SST). The SST (Logan, 1994a) engages core brain networks and RFA domains of impulsivity and impulse control (Whelan et al., 2012; Hart et al., 2012); activates key brain regions across subjects with impulsivity problems (Hart et al., 2012); shows adolescent-specific and addiction effects (Whelan et al., 2012; Smith et al., 2014); and leverages data being collected as part of IMAGEN (Whelan et al., 2012; Schumann et al., 2010).

The SST requires participants to withhold or interrupt a motor response to a "Go" stimulus when it is followed unpredictably by a signal to stop (Fig. 5). Each of 2 runs contains 180 trials. Each trial begins with the presentation of a leftward or rightward pointing arrow in black on a mid-grey background. Participants are instructed to indicate the direction of the arrow, responding "as quickly and accurately as possible" via a two-button response panel. Participants respond with their dominant hand and stimulus/response mapping is congruent with handedness. Thirty of the trials (16.67%) are "Stop" trials on which the leftward or rightward facing arrow is followed unpredictably by the "Stop Signal", that is an up-right arrow presented for 300 ms. The greater frequency of "Go" trials establishes a strong prepotent "Go" response

To ensure that there are approximately 50% successful and 50% unsuccessful inhibition trials for Stop trials, a tracking algorithm varies the interval between the onset of the leftward or rightward facing arrow and the onset of the Stop Signal (Stop Signal Delay: SSD). The initial SSD is 50 ms. Following an unsuccessful inhibition, the task is made easier by reducing the SSD by 50 ms on the next Stop trial. Following a successful inhibition, the task is made more difficult by increasing the SSD by 50 ms on the next Stop trial.

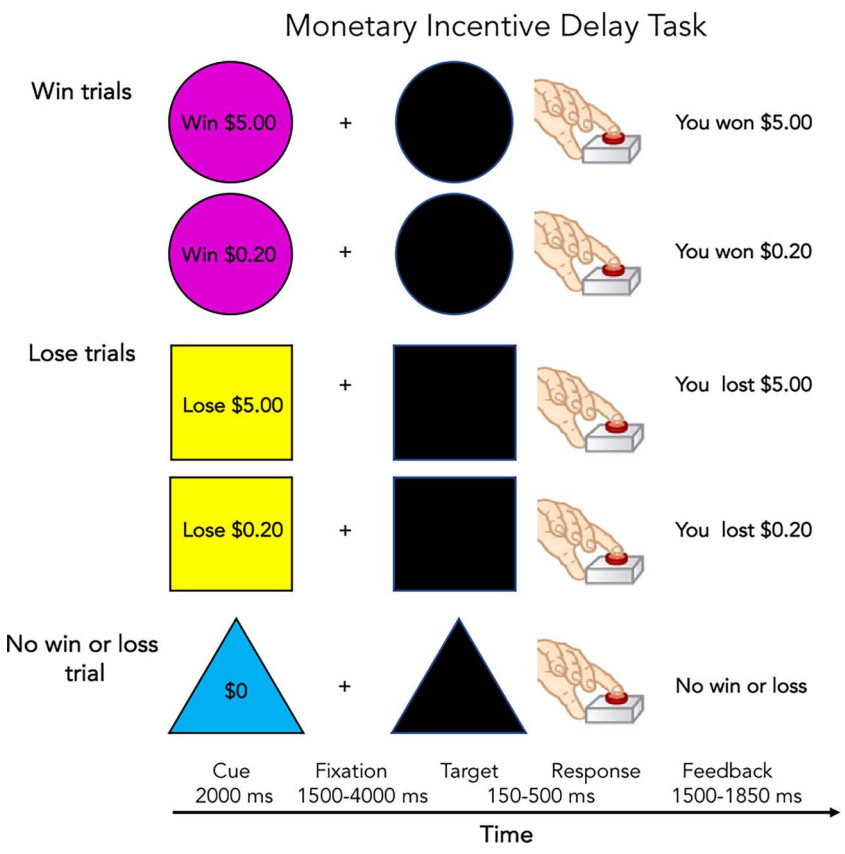

Fig. 3. Monetary incentive delay task.
(Adapted from Knutson et al., 2001)

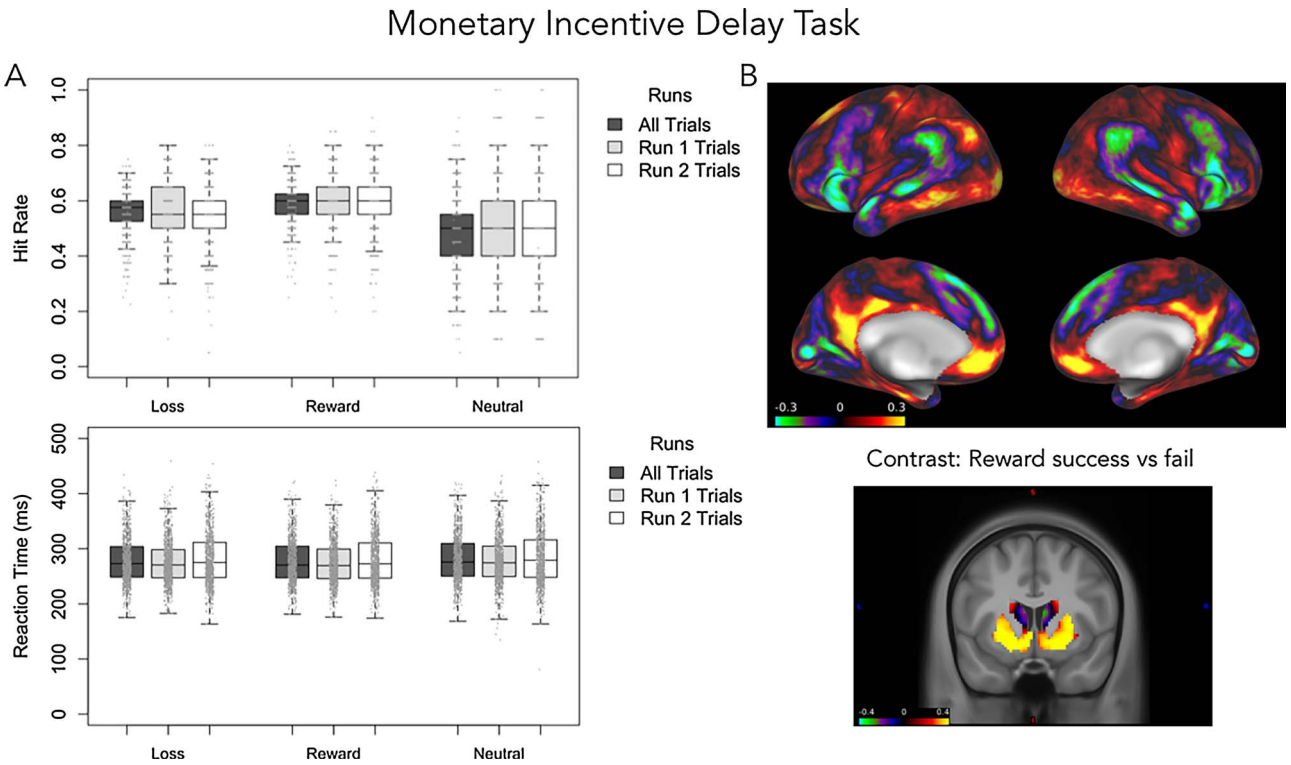

Fig. 4. Preliminary results for the MID task. A. Hit rate and reaction time are presented as a function of loss, reward and neutral trials for the first and second half of the data (Run 1 and Run 2). B. Cortical (top) and subcortical (bottom) maps for the contrast of reward success vs fail (signed Cohen's d) show reliable activation of expected brain circuitry in medial prefrontal cortex (top) and the ventral striatum (bottom).

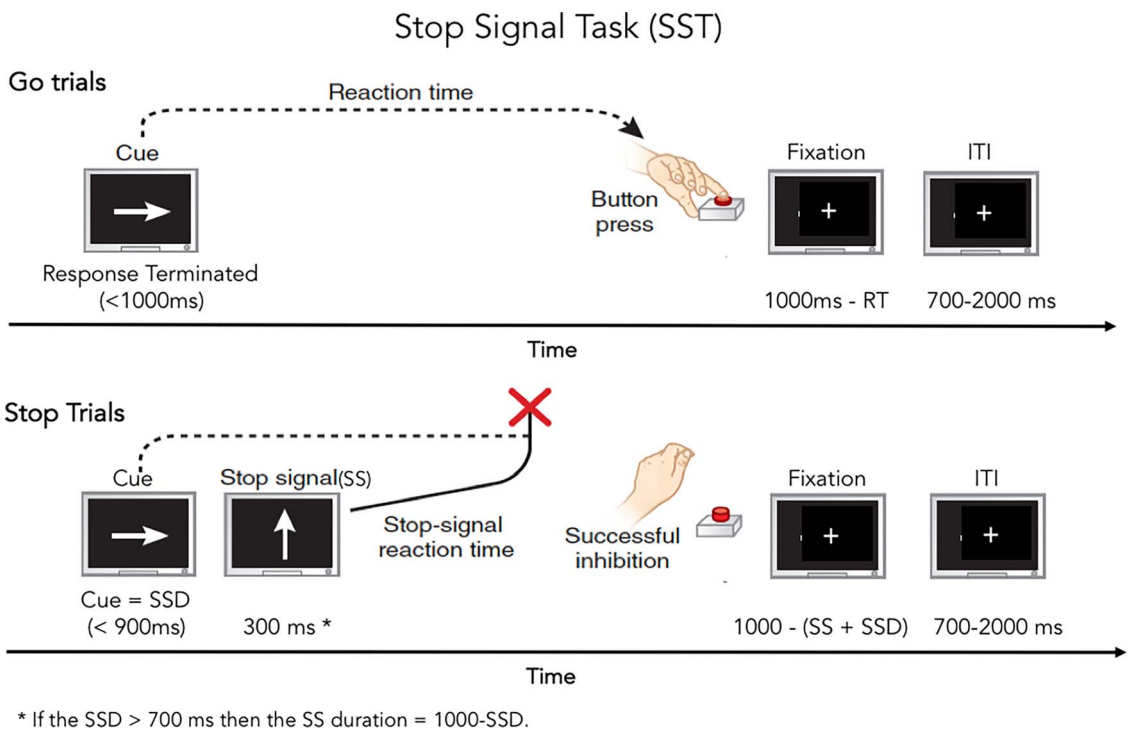

Fig. 5. Stop signal task. Examples of Go and Stop trials with timing are provided. ITI = Inter-trial interval; RT = Reaction time; SSD = Stop signal delay; SS = Stop signal. (Adapted from Helfinstein and Poldrack, 2012)

Each trial lasts 1000 ms: Go trials comprise a response terminated arrow (50% rightward facing) followed by a fixation cross of variable length for a total trial duration of 1000 ms; Stop trials comprise the arrow (50% rightward facing) presented for the duration of the SSD as determined by the algorithm followed by a 300 ms Stop Signal, and then by a fixation cross for a total duration of 1000 ms. Stimulus Onset Asynchrony (SOA) ranges from 1700 ms to 3000 ms with a mean SOA of 1904 ms. The number of Go trials separating Stop trials ranges from 1 to 20 with a mean of 4.91 trials. Each run terminates with a variable length fixation cross to bring the experimental length of each run to 349 s. The length of the final fixation cross ranges from 1038 ms to 8817 ms, with a mean of 4297.625 ms. Twelve optimized trial orders were generated, constraining the first trial of each run to be a Go trial and separating Stop trials by at least one Go trial. Stop signal reaction time (SSRT), RTs on Go trials, and accuracy are key dependent measures. In total there are 360 trials across 2 runs. Each run consists of 150 Go trials and 30 Stop trials, with the anticipation of 15 successful inhibitions and 15 failed inhibitions for a total of 300 Go trials and approximately 30 successful Stop trials and 30 failed Stop trials.

Preliminary behavioral results on the SST task (n = 965) show that the algorithm to ensure an approximately equal number of successful and unsuccessful inhibition (stop) trials is working with just over 50% stop error trials (See Fig. 6a). Accuracy on the go trials is over 80% with fewer than 20% of trials coded as incorrect due to a late response, error (i.e., pressed incorrect button) or no response. This performance is maintained across the experimental runs of the task. The SSRT appears to decrease over runs indicating improved inhibitory ability over time.

Preliminary examination of the SST imaging data look promising too. Fig. 6b depicts the signed effect sizes (Cohen's d) for the contrast of correct stop trials vs correct go trials (n = 750). There is robust activation of the lateral prefrontal cortex, anterior cingulate cortex and striatum when participants correctly inhibit a response (Fig. 6b). A key objective for the ABCD study will be to examine how behavioral and neural correlates of impulse control and impulsivity change as a function of development and substance use and abuse.

3.3.3.3. The EN-back task. The EN-back task (Fig. 6, Cohen et al., 2016a, 2016b) engages memory and emotion regulation processes and is a variant the HCP n-back task (http://www.humanconnectome.org/; Barch et al., 2013). The memory component of the n-back activates core brain networks relevant for working memory (Barch et al., 2013; Owen et al., 2005), providing evidence for its validity as a measure of working memory. It contains both high and a low memory load conditions (2 back and 0 back – see below) and the comparison of the two allows for the assessment of activation that is specifically associated with working memory as opposed to cognitive function more generally. This task shows reliable brain activations across subjects (Drobyshevsky et al., 2006) and time (Caceres et al., 2009). The task is sensitive to marijuana and alcohol use (Caldwell et al., 2005; Schweinsburg et al., 2005, 2008, 2010; Squeglia et al., 2011; Tapert et al., 2001, 2004) is developmentally appropriate (Barch et al., 2013; Casey et al., 1995) and has been widely used in the field (Owen et al., 2005), providing generalizability to other studies. Finally, this task directly builds upon data collected as part of the lifespan pilot of the Human Connectome Project (Barch et al., 2013). The stimuli, unlike the traditional or HCP versions of the n-back task, include a set of happy, fearful and neutral facial expressions (Conley et al., 2017; Tottenham et al., 2009). Cognitive processing of these stimuli taps fronto-amygdala circuitry and functions involved in emotion reactivity and regulation (Hare et al., 2008; Gee et al., 2013), and taps ventral fronto-striatal circuitry implicated in reward (Somerville et al., 2011), providing evidence of its validity as a measure of emotion reactivity. Further, the ability to contrast neural faces to the happy and fearful faces allows for an assessment of the specificity of activation to emotionally evocative stimuli. These circuits have been implicated in addiction (Koob, 2003) and show adolescent-specific brain activations (Hare et al., 2008; Dreyfuss et al., 2014). The use of place stimuli as a non-emotional and non-social set of stimuli has been shown to produce highly reliable patterns of brain activity across subjects and time (Peelen and Downing, 2005). The facial stimuli are drawn from the NimStim emotional stimulus set (Tottenham et al., 2009) and the Racially Diverse Affective Expressions (RADIATE) set of stimuli (Conley et al., 2017)

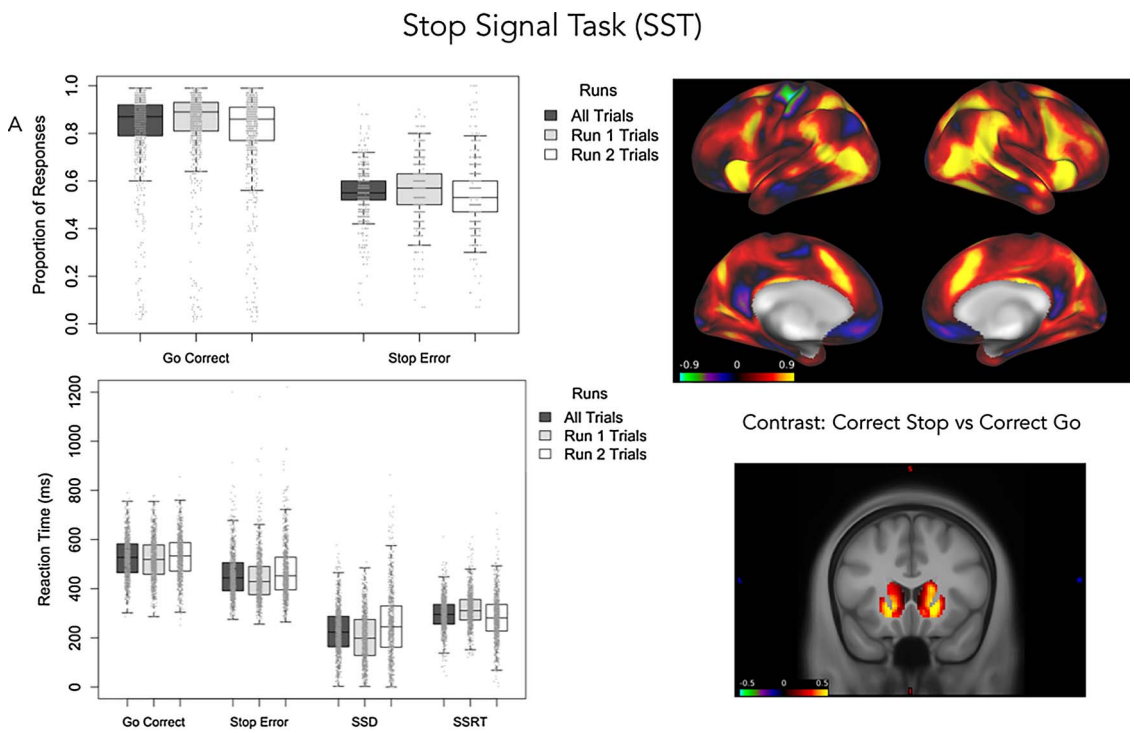

Fig. 6. Preliminary Results for the SST. A. Accuracy and reaction times are presented as function go and stop trials. B. Cortical patterns of brain activity (signed Cohen's d) for the contrast of correct stop vs correct go trials (top) and subcortical activity in the putamen for correct stop trials vs error stop trials. SSRT: stop signal reaction time; SSD: stop signal delay.

to adequately address the diversity among ABCD participants. The place stimuli are drawn from previous visual perception studies (Kanwisher, 2001; O'Craven and Kanwisher, 2000; Park and Chun, 2009).

The task includes two runs of eight blocks each. On each trial, participants are asked to respond as to whether the picture is a "Match" or "No Match." Participants are told to make a response on every trial. In each run, four blocks are 2-back conditions for which participants are instructed to respond "match" when the current stimulus is the same as the one shown two trials back. There are also four blocks of the 0-back condition for which participants are instructed to respond "match" when the current stimulus is the same as the target presented at the beginning of the block. At the start of each block, a 2.5 s cue indicates the task type ("2-back" or "target=" and a photo of the target stimulus). A 500 ms colored fixation precedes each block instruction, to alert the child of a switch in the task condition. In this emotional variant of the task, blocks of trials consist of happy, fearful, and neutral facial expressions as well as places. Accuracy for the two memory load conditions (0- and 2-back) for each stimulus type (emotional faces, neutral faces, places) and across stimulus types, are the primary dependent measures.

Each block consists of 10 trials (2.5 s each) and 4 fixation blocks (15 s each). Each trial consists of a stimulus presented for 2 s, followed immediately by a 500 ms fixation cross. Of the 10 trials in each block, 2 are targets, 2–3 are non-target lures, and the remainder are non-lures (i.e., stimuli only presented once). There are 160 trials total with 96 unique stimuli of 4 different stimulus types (24 unique stimuli per type) are presented in separate blocks in each run. For the working memory component, the main contrast is a block design analyses contrasting 2-back and 0-back (8 blocks each). For secondary event-related analyses of target trials, there are 16 targets in the 2-back and 16 in the 0-back. In sum, there are 80 trials for each of the two memory load conditions, and 20 trials for each stimulus type in each of the two memory load conditions. Thus, 40 trials of each stimulus types (Fig. 7).

Preliminary behavioral data from the EN-back task (n = 965) indicate that most participants understood and could perform the task. The median accuracy is 0.82 and this level of performance is maintained across the two experimental runs (0.81 and 0.84, respectively, Fig. 8a) showing reliability in performance across the task. Accuracy was slightly better for the no memory load (0-back) condition than the memory load (2-back) condition with the median accuracy of 0.88 and 0.78, respectively. The relatively high level of mean accuracy for this age group on a difficult task is encouraging, since unlike the MID and SST, the Emotional n-back task does not individualize task difficulty.

The preliminary imaging results (n = 517) on this task are consistent with the working memory literature (Fig. 8b). Specifically, fronto-parietal and fronto-thalamic activity previously associated with manipulation and maintenance of information in memory is observed for the main contrast of the 2-back vs the 0-back condition. A key question of the ABCD study will be how memory processes and the underlying neurocircuitry are impacted by chronic substance use during adolescence.

3.4. Post-scan assessments

3.4.1. Arousal questionnaire

Immediately following scanning, participants are administered the ABCD arousal state questionnaire again (see Supplemental Table 1), followed by an Emotional n-back Recognition Memory task (Supplemental Fig. 1) and a brief MID task questionnaire (Supplemental Table 2).

3.4.2. The EN-back recognition memory task

This task is a recognition memory test and a variant of the lifespan HCP task (http://www.humanconnectome.org/; Barch et al., 2013; Cohen et al., 2016a, 2016b; Supplemental Fig. 1A). It measures short-term memory processes that tap hippocampal functioning (Stark and Okado 2003) implicated in substance use and abuse (De Bellis et al., 2000; Medina et al., 2007). The task includes 48 old stimuli presented during the emotional n-back task and 48 new stimuli, with equal numbers of each stimulus type in the old and new stimulus sets (12 each of happy, fearful, and neutral facial expressions as well as places in each

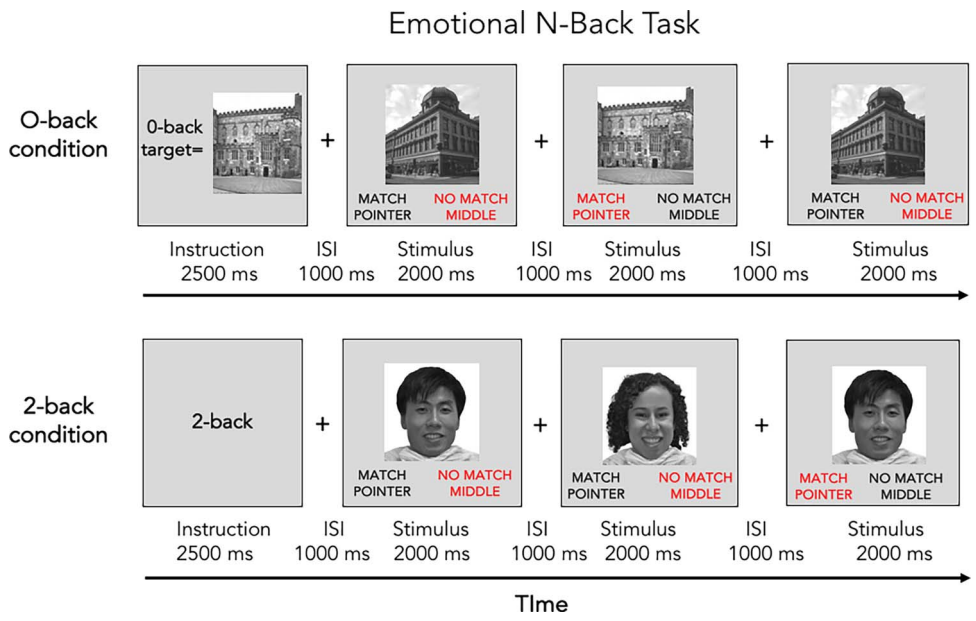

Fig. 7. Emotional N-Back Task.
(Adapted from Barch et al.2013; Cohen et al., 2016a, 2016b)

set). A total of 96 pictures are presented during the recognition memory test. Participants are asked to rate each picture as either "Old" or "New." Each picture is presented for 2 s followed immediately by a 1 s presentation of a fixation cross. Instructions and a 2-trial practice (one "Old" from the task practice and one new stimulus) precede the memory test. The task assesses memory for stimuli presented during the emotional n-back and takes approximately 5–10 min. Preliminary results (n = 868), suggest relatively low immediate recognition of

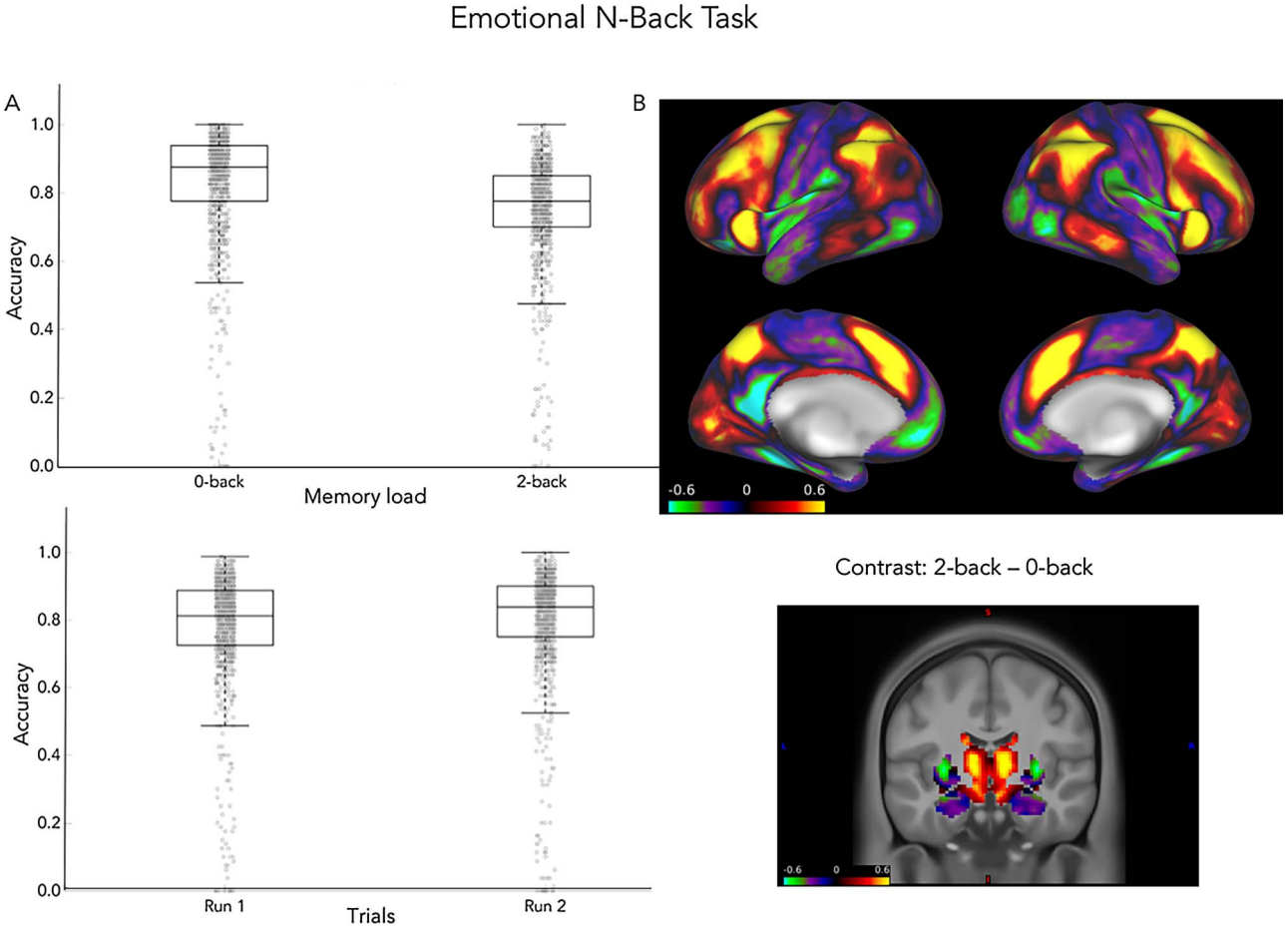

Fig. 8. Preliminary results for the Emotional n-back task. A. Behavioral results. Boxplots provide the median, first and third quartiles for accuracy on the 0-back and 2-back conditions and for each experimental run of the task. B. fMRI results. Cortical (top) and subcortical (bottom) functional maps (signed Cohen's d) for the contrast 2-back vs 0-back.

specific stimuli, especially face stimuli at this age (Supplemental Fig. 1B).

3.4.3. The monetary incentive delay task post-scan questionnaire

This questionnaire asks the participant to rate how they felt when viewing the different cues and receiving the different outcomes during the MID task to determine the effectiveness and value of wins and losses (Supplemental Table 2). This questionnaire takes approximately 1–2 min. Previous reports of ventral striatal activation by reward anticipation on the MID task have correlated with individual differences in self-reported happiness about high-reward cues (Knutson et al., 2001).

4. Conclusions

The primary objective of the ABCD study is to create a unique data resource for tracking human brain development from childhood through adolescence to determine biological and environmental factors that impact or alter developmental trajectories. This article provides an overview of imaging procedures, instrumentation and protocol that have been harmonized across all 21 ABCD sites. Preliminary examination of behavioral and imaging data demonstrate feasibility and the developmental appropriateness of the procedures and protocol as well as generalizability of the findings to the existent literature.

The ABCD Study is based on an open science model. In partnership with the NIMH Data Archive (NDA), fast-track data containing unprocessed neuroimaging data and basic participant demographics (age, sex) has been released monthly since June 2017. The ABCD Study will release curated, anonymized data including all assessment domains annually, beginning February 2018 to the research community. Information on how to access ABCD data through the NIMH Data Archive (NDA) is available on the ABCD study data sharing webpage: https://abcdstudy.org/scientists_data_sharing.html. This open science model will allow scientists from all over the world to access and analyze the data with the goal of more rapid scientific discoveries that can enhance the well-being of youth and society.

Conflicts of interest

DMB consults for Amgen, Pfizer and Upsher-Smith on work related to psychosis, JMB receives project funding from Boehringer-Ingelheim. The authors report no other conflicts of interest specific to the materials presented in this article.

Acknowledgements

This work was supported in part by U24 DA041123 (BJC, MDC, ASD, HB, DJH, JMK, JRP, CSS), U01 DA041174 (BJC, TC, DVD, MIC, MR, TT, TDW), NSF National Science Foundation Graduate Research Fellowship (AOC), U01 DA041106 (MMH, MES), U01 DA041120 (MTB, DMB, JMB, MH, NUFD, NKS, KMT), U01 DA 041156 (ASD, MCR, ARL), K01 DA037819 (MTS) U01DA041148 (HG, RW) and U24 DA041147 (HG, MHM).

Appendix A. Supplementary data

Supplementary data associated with this article can be found, in the online version, at https://doi.org/10.1016/j.dcn.2018.03.001.

References

Andrews, M.M., Meda, S.A., Thomas, A.D., Potenza, M.N., Krystal, J.H., Worhunsky, P., et al., 2011. Individuals family history positive for alcoholism show functional magnetic resonance imaging differences in reward sensitivity that are related to impulsivity factors. Biol. Psychiatry 69, 675–683.

Balodis, I.M., Potenza, M.N., 2015. Anticipatory Reward processing in addicted populations: a focus on the monetary incentive delay task. Biol. Psychiatry 77 (5), 434–444.

Barch, D.M., Burgess, G.C., Harms, M.P., Petersen, S.E., Schlaggar, B.L., et al., 2013. WU-Minn HCP Consortium (2013) Function in the human connectome: task-fMRI and individual differences in behavior. Neuroimage 80, 169–189.

Baumeister, R.F., Bratslavsky, E., Muraven, M., Tice, D.M., 1998. Ego depletion: is the active self a limited resource? J. Pers. Soc. Psychol. 74, 1252–1265. http://dx.doi.org/10.1037/0022-3514.74.5.1252.

Beck, A., Schlagenhauf, F., Wustenberg, T., Hein, J., Kienast, T., Kahnt, T., et al., 2009. Ventral striatal activation during reward anticipation correlates with impulsivity in alcoholics. Biol. Psychiatry 66, 734–742.

Bjork, J., Knutson, B., Fong, G., Caggiano, D., Bennett, S., Hommer, D., 2004. Incentive-elicited brain activation in adolescents: similarities and differences from young adults. J. Neurosci. 24, 1793–1802.

Bjork, J.M., Smith, A.R., Chen, G., Hommer, D.W., 2010. Adolescents, adults and rewards: comparing motivational neurocircuitry recruitment using fMRI. PLoS One 5 (7), e11440. http://dx.doi.org/10.1371/journal.pone.0011440.

Burgund, E.D., Kang, H.C., Kelly, J.E., Buckner, R.L., Snyder, A.Z., et al., 2002. The feasibility of a common stereotactic space for children and adults in fMRI. Neuroimage 17 (1), 184–200.

Caceres, A., Hall, D.L., Zelaya, F.O., Williams, S.C., Mehta, M.A., 2009. Measuring fMRI reliability with the intra-class correlation coefficient. Neuroimage 45, 758–768.

Caldwell, L.C., Schweinsburg, A.D., Nagel, B.J., Barlett, V.C., Brown, S.A., Tapert, S.F., 2005. Gender and adolescent alcohol use disorders on BOLD response to spatial working memory. Alcohol Alcohol. 40, 194–200.

Casey, B.J., Cohen, J.D., Jezzard, P., Turner, R., Noll, D.C., Trainor, R.J., Giedd, J., Kaysen, D., Hertz-Pannier, L., Rapoport, J.L., 1995. Activation of prefrontal cortex in children during a nonspatial working memory task with functional MRI. Neuroimage 2 (3), 221–229. http://dx.doi.org/10.1006/nimg.1995.1029. PMID: 9343606.

Cohen, A.O., Breiner, K., Steinberg, L., Bonnie, R.J., Scott, E.S., Taylor-Thompson, K.A., Rudolph, M.D., Chein, J., Richeson, J.A., Heller, A.S., Silverman, M.R., Dellarco, D.V., Fair, D.A., Galvan, A., Casey, B.J., 2016a. When is an adolescent and adult? Assessingcognitive control in emotional and non-emotional contexts. Psychol. Sci. 27 (4), 549–562.

Cohen, A.O., Conley, M.I., Dellarco, D.V., Casey, B.J., 2016b. The impact of emotional cues on short-term and long-term memory during adolescence. In: Proceedings of the Society for Neuroscience. San Diego, CA. November.

Conley, M.I., Dellarco, D.V., Rubien-Thomas, E.A., Cervera Tottenham, N., Casey, B.J., 2017. The racially diverse affective expressions (RADIATE) face set of stimuli. In: Proceedings of the Association for Psychological Science. Boston, MA.

De Bellis, M.D., Clark, D.B., Beers, S.R., Soloff, P., Boring, A.M., et al., 2000. Hippocampal volume in adolescent onset alcohol use disorders. Am. J. Psychiatry 157, 737–744.

Dosenbach, N.U.F., Koller, J.M., Earl, E.A., Miranda-Dominguez, O., Klein, R.L., Van, A.N., Snyder, A.Z., Nagel, B.J., Nigg, J.T., Nguyen, A., Wesevich, V., Greene, D.J., Fair, D.A., 2017. Real-time motion analytics during brain MRI improve data quality and reduce costs. Neuroimage 161 (Nov), 80–93. http://dx.doi.org/10.1016/j.neuroimage.2017.08.025.

Dreyfuss, M., Caudle, K., Drysdale, A.T., Johnston, N.E., Cohen, A.O., et al., 2014. Teens impulsively react rather than retreat from threat. Dev. Neurosci. 36 (3-4), 220–227. http://dx.doi.org/10.1159/000357755.

Drobyshevsky, A., Baumann, S.B., Schneider, W., 2006. A rapid fMRI task battery for mapping of visual, motor, cognitive, and emotional function. Neuroimage 31, 732–744.

Epstein, J.N., Casey, B.J., Tonev, S.T., Davidson, M., Reiss, A.L., et al., 2007. Assessment and prevention of head motion during imaging of patients with attention deficit hyperactivity disorder. Psychiatry Res.: Neuroimaging 155 (1), 75–82.

Fair, D.A., Nigg, J.T., Iyer, S., Bathula, D., Mills, K.L., Dosenbach, N.U., Schlaggar, B.L., Mennes, M., Gutman, D., Bangaru, S., Buitelaar, J.K., Dickstein, D.P., Di Martino, A., Kennedy, D.N., Kelly, C., Luna, B., Schweitzer, J.B., Velanova, K., Wang, Y.F., Mostofsky, S., Castellanos, F.X., Milham, M.P., 2012. Distinct neural signatures detected for ADHD subtypes after controlling for micro-movements in resting state functional connectivity MRI data. Front. Syst. Neurosci. 6 (80). http://dx.doi.org/10.3389/fnsys.2012.00080. PubMed PMID: 23382713; PMCID: 3563110.

Gee, D.G., Humphreys, K.L., Flannery, J., Goff, B., Telzer, E.H., et al., 2013. A developmental shift from positive to negative connectivity in human amygdala–prefrontal circuitry. J. Neurosci. 33, 4584–4593.

Hare, T.A., Tottenham, N., Galvan, A., Voss, H.U., Glover, G.H., Casey, B.J., 2008. Biological substrates of emotional reactivity and regulation in adolescence during an emotional go-nogo task. Biol. Psychiatry 63, 927–934.

Hart, H.R.J., Nakao, T., Mataix-Cols, D., Rubia, K., 2012. Meta-analysis of functional magnetic resonance imaging studies of inhibition and attention in attention-deficit/hyperactivity disorder: exploring task-specific, stimulant medication, and age effects. JAMA Psychiatry 70 (2), 185–198.

Heitzeg, M.M., Villafuerte, S., Weiland, B.J., Enoch, M.A., Burmeister, M., et al., 2014. Effect of GABRA2 genotype on development of incentive-motivation circuitry in a sample enriched for alcoholism risk. Neuropsychopharmacology 39 (13), 3077–3086.

Helfinstein, S.M., Poldrack, R.A., 2012. (2012), The young and the reckless. Nat. Neurosci. 15 (6), 803–805. http://dx.doi.org/10.1038/nn.3116. May 25.

Holland, D., Kuperman, J.M., Dale, A.M., 2009. Efficient correction of inhomogeneous static magnetic field-induced distortion in echo planar imaging. Neuroimage 50 (1).

Jernigan, T.L., et al., 2016. The pediatric imaging, neurocognition, and genetics (PING) data repository. Neuroimage 124 (Pt B), 1149–1154.

Kang, H.C., Burgund, E.D., Lugar, H.M., Petersen, S.E., Schlaggar, B.L., 2003. Comparison of functional activation foci in children and adults using a common stereotactic space. Neuroimage 19 (1), 16–28.

Kanwisher, N., 2001. Neural events and perceptual awareness. Cognition 79 (1), 89–113.

Knutson, B., Westdorp, A., Kaiser, E., Hommer, D., 2000. FMRI visualization of brain activity during a monetary incentive delay task. Neuroimage 12, 20–27.

Knutson, B., Adams, C.M., Fong, G.W., Hommer, D., 2001. Anticipation of increasing monetary reward selectively recruits nucleus accumbens. J. Neurosci. 21 (16), RC159 Aug 15.
Koob, G.F., 2003. Neuroadaptive mechanisms of addiction: studies on the extended amygdala. Eur. Neuropsychopharmacol. 13, 442–452.
Logan, G.D., 1994a. On the ability to inhibit thought and action: a users' guide to the stop signal paradigm. In: Dagenbach, D., Carr, T.H. (Eds.), Inhibitory Processes in Attention, Memory, and Language. Academic Press, San Diego, pp. 189–239.
Logan, G.D., 1994b. Spatial attention and the apprehension of spatial relations. J. Exp. Psychol.: Hum. Percept. Perform. 20, 1015–1036.
Medina, K.L., Schweinsburg, A.D., Cohen-Zion, M., Nagel, B.J., Tapert, S.F., 2007. Effects of alcohol and combined mar ijuana and alcohol use during adolescence on hippocampal volume and asymmetry. Neurotoxicol. Teratol. 29 (1), 141–152.
O'Craven, K.M., Kanwisher, N., 2000. Mental imagery of faces and places activates corresponding stimulus-specific brain regions. J. Cogn. Neurosci. 12 (6), 1013–1023.
Owen, A.M., McMillan, K.M., Laird, A.R., Bullmore, E., 2005. N-back working memory paradigm: a meta-analysis of normative functional neuroimaging studies. Hum. Brain Mapp. 25 (1), 46–59.
Park, S., Chun, M.M., 2009. Different roles of the parahippocampal place area (PPA) and retrosplenial cortex (RSC) in panoramic scene perception. Neuroimage 47 (4), 1747–1756.
Peelen, M.V., Downing, P.E., 2005. Within-subject reproducibility of category-specific visual activation with functional MRI. Hum. Brain Mapp. 25 (4), 402–408.
Power, J.D., Barnes, K.A., Snyder, A.Z., Schlaggar, B.L., Petersen, S.E., 2012. Spurious but systematic correlations in functional connectivity MRI networks arise from subject motion. Neuroimage 59 (3), 2142–2154.
Power, J.D., Mitra, A., Laumann, T.O., Snyder, A.Z., Schlaggar, B.L., Petersen, S.E., 2013. Methods to detect, characterize, and remove motion artifact in resting state fMRI. Neuroimage 84, 048. http://dx.doi.org/10.1016/j.neuroimage. 2013.08.048. PubMed PMID: 23994314; PMCID: 3849338.
Rosenberg, M., Casey, B.J., Holmes, A., 2018. Prediction complements explanation in understanding the developing brain. Nat. Commun. 9, 589. http://dx.doi.org/10.1038/s41467-018-02887-9.
Satterthwaite, T.D., Wolf, D.H., Loughead, J., Ruparel, K., Elliott, M.A., Hakonarson, H., Gur, R.C., Gur, R.E., 2012. Impact of in-scanner head motion on multiple measures of functional connectivity: relevance for studies of neurodevelopment in youth. Neuroimage 60 (1), 623–632. http://dx.doi.org/10.1016/j.neuroimage.2011.12.063. Epub 2012/01/12. S1053-8119(11)01465-0 [pii] . PubMed PMID: 22233733; PMCID: 3746318.
Schumann, G., Loth, E., Banaschewski, T., Barbot, A., Barker, G., Büchel, C., Conrod, P.J., Dalley, J.W., Flor, H., Gallinat, J., Garavan, H., Heinz, A., Itterman, B., Lathrop, M., Mallik, C., Mann, K., Martinot, J.L., Paus, T., Poline, J.B., Robbins, T.W., Rietschel, M., Reed, L., Smolka, M., Spanagel, R., Speiser, C., Stephens, D.N., Ströhle, A., Struve, M., 2010. IMAGEN consortium. The IMAGEN study: reinforcement-related behaviour in normal brain function and psychopathology. Mol. Psychiatry 15 (December (12)), 1128–1139.
Schweinsburg, A.D., Schweinsburg, B.C., Cheung, E.H., Brown, G.G., Brown, S.A., Tapert, S.F., 2005. fMRI response to spatial working memory in adolescents with comorbid marijuana and alcohol use disorders. Drug Alcohol Depend. 79, 201–210 A.i.31.
Schweinsburg, A.D., Nagel, B.J., Schweinsburg, B.C., Park, A., Theilmann, R.J., Tapert, S.F., 2008. Abstinent adolescent marijuana users show altered fMRI response during spatial working memory. Psychiatry Res.: Neuroimaging 163, 40–51 (A.i.47).
Schweinsburg, A.D., Schweinsburg, B.C., Medina, K.L., McQueeny, T., Brown, S.A., Tapert, S.F., 2010. The influence of recency of use on fMRI response during spatial working memory in adolescent marijuana users. J. Psychoact. Drugs 42, 401–412 A.i.74.
Smith, J.L., Mattick, R.P., Jamadar, S.D., Iredale, J.M., 2014. Deficits in behavioural inhibition in substance abuse and addiction: a meta-analysis. Drug Alcohol Depend. 145, 1–33.
Somerville, L.H., Hare, T., Casey, B., 2011. Frontostriatal maturation predicts cognitive control failure to appetitive cues in adolescents. J. Cognit. Neurosci. 23 (9), 2123–2134. http://dx.doi.org/10.1162/jocn.2010.21572.
Squeglia, L.M., Dager Schweinsburg, A., Pulido, V., Tapert, S.F., 2011. Adolescent binge drinking linked to abnormal spatial working memory brain activation: differential gender effects. Alcohol.: Clin. Exp. Res. 35, 1–11 A.i.86.
Stark, C.E., Okado, Y., 2003. Making memories without trying: medial temporal lobe activity associated with incidental memory formation during recognition. J. Neurosci. 23, 6748–6753.
Tapert, S.F., Brown, G.G., Kindermann, S., Cheung, E., Frank, L.R., Brown, S.A., 2001. fMRI measurement of brain dysfunction in alcohol dependent young women. Alcohol.: Clin. Exp. Res. 25, 236–245.
Tapert, S.F., Schweinsburg, A.D., Barlett, V.C., Meloy, M.J., Brown, S.A., Brown, G.G., Frank, L.R., 2004. Blood oxygen level dependent response and spatial working memory in adolescents with alcohol use disorders. Alcohol.: Clin. Exp. Res. 28, 1577–1586 A.i.24.
Tisdall, M.D., Hess, A.T., Reuter, M., Meintjes, E.M., Fischl, B., van der Kouwe, A.J.W., 2012. Volumetric navigators for prospective motion correction and selective reacquisition in neuroanatomical MRI. Magn. Reson. Med. 68 (2), 389–399 (PMID: 22213578.
Tottenham, N., Tanaka, J., Leon, A.C., McCarry, T., Nurse, M., et al., 2009. The NimStim set of facial expressions: judgments from untrained research participants. Psychiatry Res. 168 (3), 242–249.
Treiber, J.M., White, N.S., Steed, T.C., Bartsch, H., Holland, D., Farid, N., et al., 2016. Characterization and correction of geometric distortions in 814 diffusion weighted images. PLoS One 11 (3), e0152472. http://dx.doi.org/10.1371/journal.pone.0152472.
Van Dijk, K.R., Sabuncu, M.R., Buckner, R.L., 2012. The influence of head motion on intrinsic functional connectivity MRI. Neuroimage 59 (1), 431–438.
Villafuerte, S., Heitzeg, M.M., Foley, S., Yau, W.Y.W., Majczenko, K., et al., 2012. Impulsiveness and insula activation during reward anticipation are associated with genetic variants in GABRA2 in a family sample enriched for alcoholism. Mol. Psychiatry 17, 511–519.
Villafuerte, S., Trucco, E.M., Heitzeg, M.M., Burmeister, M., Zucker, R.A., 2014. Genetic variation in GABRA2 moderates peer influence on externalizing behavior in adolescents. Brain Behav. 4 (6), 833–840. http://dx.doi.org/10.1002/brb3.291.
Whelan, R., Conrod, P.J., Poline, J.B., Lourdusamy, A., Banaschewski, T., et al., 2012. Adolescent impulsivity phenotypes characterized by distinct brain networks. Nat. Neurosci. 15 (6), 920–925.
White, N., Roddey, C., Shankaranarayanan, A., Han, E., Rettmann, D., Santos, J., Dale, A., et al., 2010. PROMO –real-time prospective motion correction in MRI using image-based tracking. Magn. Reson. Med. 63 (1), 91–105.
Wrase, J., Schlagenhauf, F., Kienast, T., Wustenberg, T., Bermpohl, F., Kahnt, T., et al., 2007. Dysfunction of reward processing correlates with alcohol craving in detoxified alcoholics. Neuroimage 35, 787–794.
Yan, C.G., Cheung, B., Kelly, C., Colcombe, S., Craddock, R.C., Di Martino, A., Li, Q., Zuo, X.N., Castellanos, F.X., Milham, M.P., 2013a. A comprehensive assessment of regional variation in the impact of head micromovements on functional connectomics. Neuroimage 76, 183–201. http://dx.doi.org/10.1016/j.neuroimage.2013.03.004. PubMed PMID: 23499792; PMCID: 3896129.
Yan, C.G., Craddock, R.C., He, Y., Milham, M.P., 2013b. Addressing head motion dependencies for small-world topologies in functional connectomics. Front. Hum. Neurosci. 7 (910). http://dx.doi.org/10.3389/fnhum.2013.00910. PubMed PMID: 24421764; PMCID: 3872728.
Yau, W.Y., Zubieta, J.K., Weiland, B.J., Samudra, P.G., Zucker, R.A., Heitzeg, M.M., 2012. Nucleus accumbens response to incentive stimuli anticipation in children of alcoholics: relationships with precursive behavioral risk and lifetime alcohol use. J. Neurosci. 32 (7), 2544–2551.